RSC Advances

RSC Advances

www.rsc.org/advances

ROYAL SOCIETY OF CHEMISTRY

www.rsc.org/advances

In-Situ Formation of Reverse Polymeric Micelles in Liquid Alkanes to Lodge Alcohol Micro-droplets

Yeap-Hung Ng,[a] Siok Wei Tay,[b] Richard S. Hong,[b] Liang Hong[a,b]*

[a] Department of Chemical & Biomolecular Engineering, National University of Singapore, 10 Kent Ridge Crescent, Singapore 119260, Singapore

[b] Institute of Materials Research and Engineering, 3 Research Link, Singapore 117602, Singapore

Table of Content Entry

We report the *in-situ* generation of polymeric micellar solution in non-polar solvent, that allows the incorporation of oxygenate into diesel.
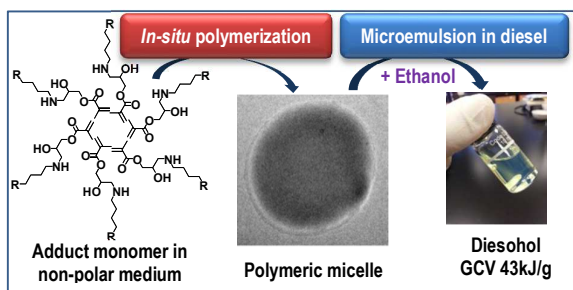
RSC Advances

ARTICLE

In-situ Formation of Reverse Polymeric Micelles in Liquid Alkanes to Lodge Alcohol Micro-droplets

Yeap-Hung Ng,[a] Siok Wei Tay,[b] Richard S. Hong,[b] Liang Hong*[a,b]

An amphiphilic comb-like polymer has been synthesized in a liquid alkane medium, which involves the alkylation of glycidyl methacrylate (GMA) by 1-hexadecylamine (HDA) or 1-octadecylamine (ODA) and the *in-situ* polymerization of the resulting alkyl methacrylate monomer. The resulting macromolecules possess a hydrophilic backbone with thickly anchored –OH and >NH groups and long aliphatic side chains extending into the alkane medium and hence undergo self-assembly in the non-polar medium. The resulting polymeric micellar solution displays an enhanced capability to dissolve methanol or ethanol than those employing low molecular weight surfactants, such as Span® 80, according to the stability study of the resulting microemulsions. The ethanol content can be raised from the contemporary level of 15% to 23% on the same loading (by weight) of emulsifier. By the ASTM D240-09 method, the in-house formulated model diesohol (diesel/ethanol/emulsifier = 75/20/5) exhibits only a minute decline in calorific value, as compared with the pristine diesel fuel.

Introduction

The major pollutants in exhaust gas from diesel engines consist of particulate matter, smoke density, oxides of nitrogen, polycyclic aromatic hydrocarbons and other emissions, posing health hazards.[1,2] It is therefore imperative to enhance the burning efficiency of diesel towards the complete combustion. This has been pursued by structural modification of diesel engine and introduction of pertinent oxygenates into diesel fuel to curb carbon-rich particles. Ethanol is a promising oxygenate additive for diesel because it is a mass petrochemical product and can also be obtained from renewable biomass resources. Furthermore, it also possesses a high gross calorific value.[3-5] As remarked by Durgun et al.,[6] there are three approaches developed thus far to improve combustion of diesel by ethanol: (1) ethanol fumigation using carburetion or manifold injection technique,[7] (2) dual fuel injection technique, and (3) forming a microemulsion in which the ethanol is highly dispersed in diesel in the presence of an appropriate emulsifier or a co-solvent. Of the three approaches, the last one is most attractive because no engine modification is required.

Physical and chemical properties affecting miscibility between ethanol and diesel have been extensively investigated by various research groups.[8-10] To improve the solubility of ethanol in diesel fuel, ethyl acetate has also been used as a co-solvent in ethanol-based microemulsified fuel as reported by Chandra[11] and Ashok et al.[12] The performance and emissions of the resultant blends were assessed in the unmodified compression-ignition (CI) engine, which shows reduced values of the air pollutants of concern. Light-scattering investigation on the formation of microemulsion in an ethanol-diesel blend reported by Loh et al.[13] provides an insight into colloidal stability of the fuel containing amphiphilic molecules, such

as dodecylamine and oleic acid. Commercially available additives such as sorbitan ester (Span® 80) and soybean methyl esters (AEP-102) have been utilized by Reyes et al. as ethanol-diesel miscibility promoters.[14] Following that, there are numerous publications focusing on the ethanol-biodiesel-diesel microemulsions, which are also termed as EB-diesel. The trans-esterified methyl esters of soybean oil, palm oil and rapeseed oil, i.e. biodiesel, were identified as the non-fossil-fuel additives since they promote ethanol-diesel miscibility as well.[15-20] On the basis of these accomplishments, exploring an oil-soluble polymeric emulsifier for a greater dissolution capacity is of interest from both fundamental and application perspectives.

Although the use of polymeric emulsifiers to stabilize o/w emulsion has been extensively studied and some of them are on market, such as Poloxamer type (e.g., Pluronic™) and acrylic type (e.g., Pemulen™), their counterpart to stabilize the reverse emulsion (w/o), in particular, in nonpolar organic medium is still rare. An *ex-situ* synthesized hydrophobic polymeric emulsifier is normally difficult to be dissolved in a non-polar organic medium because of the weak solvation capability of the nonpolar organic solvent, such as diesel or kerosene. The *in-situ* strategy is therefore an effective strategy to circumvent this thermodynamic barrier ($\Delta H > 0$) of dissolution. Carrying out polymerization of an amphiphilic monomer in a nonpolar organic solvent could avoid the dissolution step. This design is similar to the concept described in the review article by Richez et al.,[21] which summarizes the versatility of dispersion polymerization in non-polar media. A typical structure of such amphiphilic monomer consists of a vinyl group with adjacent hydrophilic groups and a long aliphatic chain. This type of molecules will undertake micellization in a non-polar solvent with their vinyl groups collecting around the core of micelles formed, in which the spatial proximity favors polymerization.
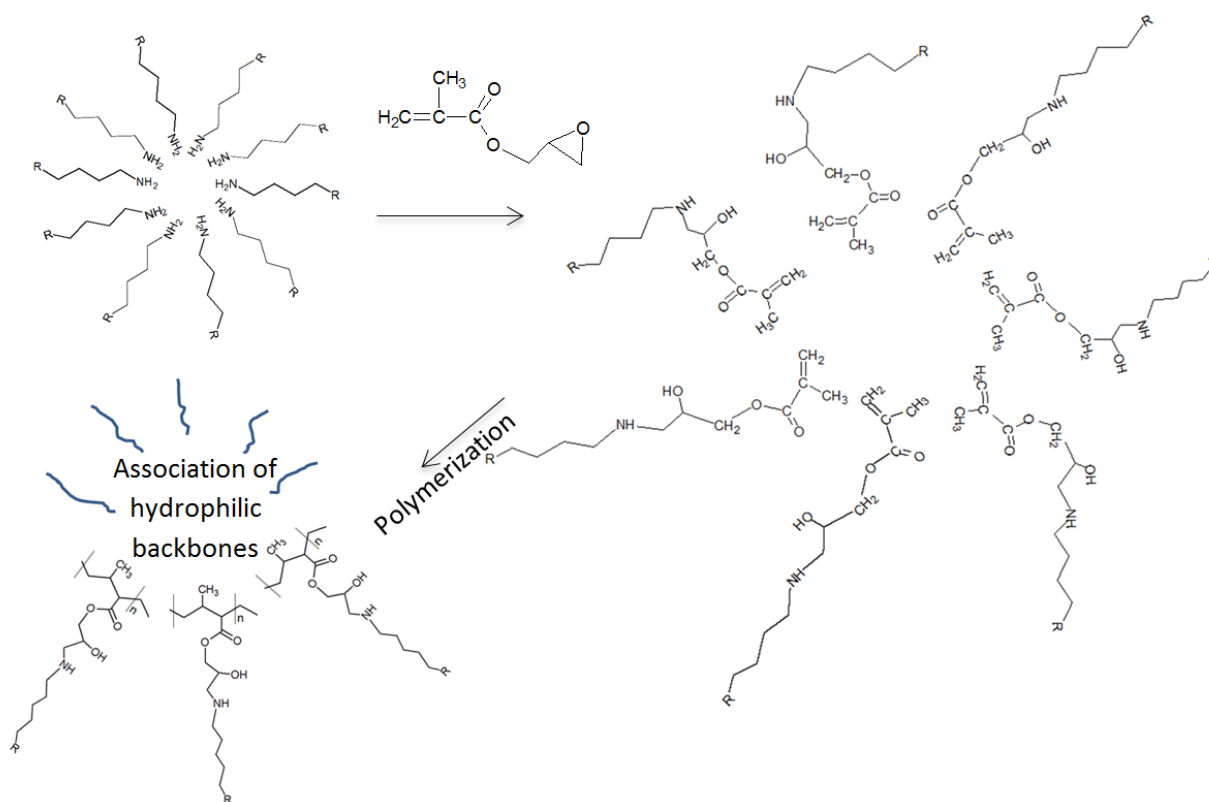
Scheme 1 *In-situ* free-radical polymerization of the adduct monomer in an alkane medium brings about a reverse polymer micellar solution.

In this study we synthesized an amphiphilic comb-like polymer in *n*-dodecane or diesel *via* free-radical polymerization of an adduct monomer derived from the ring opening alkylation of glycidyl methacrylate with a long-chain aliphatic 1-amine. As the vinyl group and hydrophilic –OH / >NH groups are regio-nearby in the adduct monomer, a polar inner space is formed inside each aggregation micelle, which facilitates polymerization as illustrated in Scheme 1. A homogeneous solution was then obtained. It is important to note that the polymer separated from the solution cannot be re-dissolved at all albeit it could be slightly dissolved in polar solvents, e.g. toluene and DMF, to just meet the needs for NMR and SEC characterizations. Such irreversibility justifies the *in-situ* synthesis as the sole route for the application of oleophilic polymer emulsifier. Moreover, the present polymerization system also permits copolymerization of the adduct monomer with the PEGylated methacrylate for instance to tune the hydrophilic trait of the core of the polymeric micelle. Subsequently, the capability of the as-generated polymeric micellar solution in *n*-dodecane (5 % by weight) to dissolve methanol or ethanol was evaluated through inspecting the change in the turbidity of the mixture. Fundamentally, turbidity is a light scattering-based measurement, detecting the occurrence of phase separation when larger and more emulsion particles are formed. We formulated an in-house model of diesohol through utilizing the polymeric micelles to lodge ethanol in the ExxonMobil synergy diesel fuel and their gross calorific values were determined by following the corresponding ASTM standard.

Experimental

1. Materials

1-Hexadecylamine (HDA, technical grade, 90%, Aldrich), 1-octadecylamine (ODA, technical grade, 90%, Aldrich), *n*-dodecane (> 99%, Sigma-Aldrich), 2,2'-azobis(isobutyronitrile) (AIBN, 0.2 M in toluene, Aldrich), toluene (analytical reagent grade, 99.99%, Fisher Chemical), ethanol (analytical reagent grade, 99.99%, Fisher Chemical), methanol (analytical reagent grade, 99.99%, Fisher Chemical), methyl ethyl ketone (MEK, 99%, Sigma-Aldrich), chloroform-*d* (99.96 atom % D, contains 0.03% v/v TMS, Aldrich) and toluene-*d*₈ (99.6 atom % D, Aldrich), commercial diesel fuel (ExxonMobil Synergy Diesel) and Span® 80 (Fluka) were used as received. Glycidyl methacrylate (GMA, 97%, Aldrich), poly(ethylene glycol) methyl ether methacrylate (PEGME-MA300, average M_n 300, Aldrich) and poly(ethylene glycol) methacrylate (PEG-MA360, average M_n 360, Aldrich) were passed through a short column of neutral alumina to remove the inhibitor before used.

2. Synthesis of the amphiphilic comb-like polymer

For a model synthesis, HDA (3.54 g, 14.66 mmol) or ODA (3.95 g, 14.66 mmol) and *n*-dodecane (15 mL) were added to a one-neck round bottom flask equipped with a magnetic stirrer and then sealed with a rubber septum. The mixture was heated to 70 °C in an oil bath for about 20 min to form a clear solution. GMA (2 mL, 14.66 mmol) was then introduced using a syringe into the solution. The mixture was stirred at 70 °C for 24 h to complete the synthesis of the respective adduct monomer, GMA-HDA and GMA-ODA. The

functional group conversion was examined using the FT-IR spectroscopy. Subsequently, the reaction mixture was diluted with 25 mL n-dodecane and purged by argon for 20 min before AIBN initiator (1 mol% with respect to GMA) was introduced into this monomer solution. The solution was then stirred at 70 °C for 24 h under argon atmosphere to complete the polymerization of the adduct monomer. Through the same procedure, three homogeneous polymeric micellar solutions (P1 – P3, Table 1) were achieved. Similarly, ExxonMobil Synergy Diesel was also used as dispersion medium in place of n-dodecane to obtain two additional polymeric micellar solutions (P4 – P5). The polymers generated were sampled respectively by withdrawing a small portion of solution and adding in excess ethanol to precipitate the polymer for structural characterizations.

Table 1 A list of the comb-like polymers and the corresponding micellar solutions

Polymeric micellar solution	Forming adduct monomer of comb-like polymer		Dispersion medium
	1-aliphatic amine	Vinyl monomer	
P1	HDA	GMA	n-dodecane
P2	ODA	GMA	n-dodecane
P3[a]	HDA	GMA	n-dodecane
P4	HDA	GMA	Diesel
P5	ODA	GMA	Diesel
P6[b]	HDA	GMA + PEGME-MA300	Diesel
P7	HDA	GMA + PEG-MA360	Diesel
P8	ODA	GMA + PEGME-MA300	Diesel
P9	ODA	GMA + PEG-MA360	Diesel

[a.] GMA/HDA=1/0.8 (molar basis); [b.] GMA/PEGME-MA300=GMA/PEG-MA360=4/1 (molar basis).

3. Incorporation of PEGylated monomer unit into the polymeric micelles

In a model synthesis, the random copolymer consisting of an adduct monomer (e.g., GMA-HDA) and a PEGylated monomer was synthesized. To realize this design, the above protocol was slightly modified by introducing PEGME-MA300 (0.84 mL, 2.93 mmol) together with 25 mL diesel into the solution of the monomer adduct after it had been synthesized in diesel. The successive steps were kept the same as described in Section 2. Correspondingly, PEG-MA360 could also be assimilated into the comb-like copolymer through the same procedure.

4. Grafting homopolymer PGMA with HDA to prepare a control sample

Free-radical polymerization of GMA in 1,4-dioxane containing AIBN (1 mol% of the monomer) was carried out at 70 °C under argon atmosphere for 6 h. The resulting homopolymer PGMA was separated from the reaction mixture by precipitation in a large excess of methanol, followed by vacuum drying at 50 °C. The recovered amount showed 93% yield. A given amount of PGMA (1 g) was dissolved in 50 mL of toluene or MEK, together with equimolar HDA based on functional group of both types. The solution was refluxed under argon for 24 h to carry out ring opening alkylation.

5. Reverse emulsion by dissolving alcohol in the polymeric micellar solution

The as-prepared polymeric micellar solution was mixed with a given amount of n-dodecane to dilute the polymeric micelles to 5 wt.%. After that, methanol was injected by portion (20 μL for each addition) into the diluted micellar solution (6.5 g) with magnetic stirring at 200 rpm for 10 min to homogenize the blend. The homogeneity of the resulting solution was monitored using a turbidity meter. In this examination, the initial turbidity was taken from the micellar solution, i.e. prior to the addition of methanol. The turbidity underwent continuous and minor variation with the introduction of alcohol by the above procedure before the incipient phase instability that accompanies a turbidity jump. As such, the alcohol solubility limit in wt.% was the alcohol added until the injection right before the injection that causes instant turbidity jump. It is clear that the comb-like polymers possess different methanol dissolution capacities, which are summarized in Table 2. Moreover, the diesel-based polymeric micellar solutions (P4 to P9) were diluted by the diesel and their alcohol- acceptances were assessed by ethanol using the same procedure as stated above (Table 3). The pristine diesel (Control 1) and Span® 80 (5 wt.%)-diesel (Control 2) were adopted respectively as control samples in this assessment.

Table 2 Formation of the reverse microemulsions[a] through dissolving methanol in the polymeric micellar solutions

Reverse microemulsion	Polymeric micellar solution	Solubility limit (wt.% MeOH)[b]	Turbidity at phase separation (NTU)
S_m1	P1	3.5	2.01
S_m2	P2	3.3	5.50
S_m3	P3	3.1	6.17
S_m4	P4	3.1	1194
S_m5	P5	3.1	1091
S_m6	P6	2.8	800
S_m7	P7	2.4[c]	NA
S_m8	P8	3.1	1246
S_m9	P9	1.7[c]	NA

[a.] Determined by the turbidity measurement. [b.] Refer to Fig. 4-5.
[c.] Flocculation of polymer P7 and P9 in the diesel happens prior to methanol phase separation (or broken of microemulsion).

Table 3 A summary of the ethanol dissolution capacity in the diesel with the use of different emulsifiers

| Reverse emulsion[a]	Emulsifier	Emulsifier wt.%	Solubility limit (wt.% EtOH)	Turbidity at phase separation (NTU)
Control 1	NIL	0	11.2	1254
Control 2	Span® 80	5	13.4	1068
S_e4_1	P4	1	12.7	806
$S_e4\_2.5$	P4	2.5	16.3	1377
S_e4	P4	5	22.6	2522
S_e5_1	P5	1	13.4	938
$S_e5\_2.5$	P5	2.5	16.3	1368
S_e5	P5	5	23.1	2394
S_e6	P6	5	19.5	1957
S_e8	P8	5	19.5	942

6. Structural and property characterizations

The purified polymer samples were characterized by ^{1}H NMR spectroscopy on a Bruker Ultra Shield spectrometer (400 MHz), using chloroform-*d* (for PGMA) and toluene-*d*$_8$ (for the comb-like polymer) as solvents. The chemical shifts were referred to the TMS peak at δ= 0.00 ppm for CDCl$_3$ and δ= 2.09 ppm for solvent peak of toluene-*d*$_8$. The FTIR spectra were obtained from a Bio-Rad Excalibur FTS-3500 FTIR spectrometer. The dissolution extent of alcohol in the polymeric micellar solution was recorded using LaMotte LTC3000 bench-top turbidity meter equipped with five measurement ranges (0-11, 11-110, 110-300, 300-600, 600-4000 NTU), which were calibrated with five respective EPA compliance turbidity standards, for example, the standard with 1000 NTU was used to check readings from the highest range. The rheological behaviors of the diesel-based polymeric micellar solution and the reverse microemulsion were characterized using Brookfield RV DV-II+ Pro Viscometer at room temperature. The PGMA and P(GMA-HDA) isolated from P1 were characterized by size exclusion chromatography (SEC) system equipped with a Waters 1515 Isocratic HPLC pump, a 717plus autosampler, a 2414 refractive-index detector, and a PLgel 5μm Mixed-D SEC column (Agilent Technologies) using DMF as an eluent, operated at 1 mL/min and 35 °C. Thermogravimetric analysis (TGA) of the pristine diesel and a selected diesel-based polymeric micellar solution was performed on TA Instrument (Q500 Thermogravimetric Analyzer). All tests were conducted under airflow (60 mL/ min) over a temperature range of 30–600 °C at a scan rate of 10 °C/min. The size distribution of micelles and emulsion particles in nonpolar media was determined using light-scattering measurement (Brookhaven 90Plus Particle Size Analyzer), with a scattering angle of 90 degree. The laser source is a semiconductor laser diode, wavelength 659 nm and laser power of 35mW. To obtain images of the polymeric micelles and the droplets of the reverse emulsion, the characterization was performed on a High-resolution Transmission Electron Microscope

(Philips CM300 FEGTEM). The polymeric micellar solution (P1) and the reverse microemulsion (20al/S_e4 in Table 4) were diluted respectively in *n*-heptane to make 0.5 wt.% colloidal dispersions. A drop of liquid was transferred from each of the dispersion to a TEM copper grid. Upon drying under ambient condition, the samples were ready for TEM. The selected ethanol-in-diesel emulsions were sent to Intertek Testing Services (Singapore) Pte Ltd to measure the gross calorific values (GCV) of them using the ASTM D240-09 standard.

Results and discussion

1. Solvent effect on the synthesis of the comb-like polymer imparted by the spectroscopic characterizations

As illustrated in Scheme 1, the ring-opening alkylation of GMA with 1-alkylamine produces the adduct monomer. The alkylation becomes solvent-selective for the long aliphatic chain of amine. Infrared (IR) spectroscopic study shows an obviously higher alkylation extent for the reaction carried out in *n*-dodecane than in toluene (Fig. 1b vs. 1c) under the same synthesis condition. The amplitude of the C=O stretching band at 1718 cm^{-1} of the GMA-HDA adduct monomer is a clear indication of the alkylation extent since the unreacted GMA has been removed from the reaction product by vacuum vaporization.
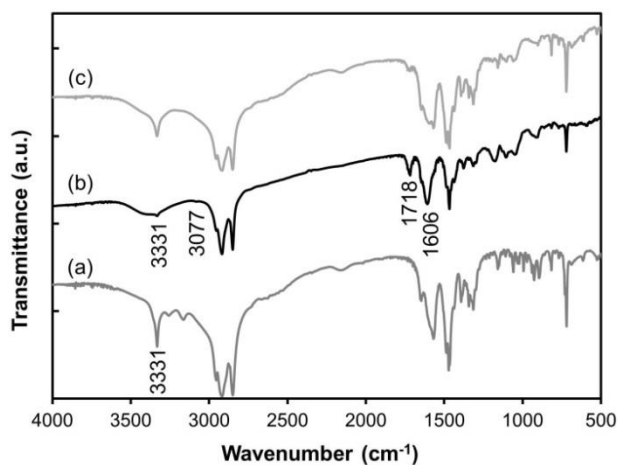
Fig. 1 FTIR spectra of (a) hexadecylamine (HDA), (b) the GMA-HDA adduct monomer synthesized in *n*-dodecane, and (c) the same adduct monomer synthesized in toluene.

In addition, compared with HDA, GMA-HDA exhibits a far weaker N-H stretching vibrations (~3331 cm^{-1}) on top of the broad –OH stretching band (3700-3500 cm^{-1}), the presence of the conjugated C=C stretching vibration at 1606 cm^{-1} and the alkene C-H stretch at 3077 cm^{-1} (Fig. 1b). All these validate the formation of the adduct product. The 1-amine could achieve maximum stretch in *n*-dodecane due to their similar molecular chain structures besides the amino end group. This also facilitates a reverse micellization in which the polar 1-amino groups assemble to form the inner core of micelle. The inner core functions as the preferential location for GMA molecules added in the micellar solution because of a large contrast of polarity between the core of micelles and the dispersion medium. This polar enrichment creates spatial proximity between the amino groups and the epoxide groups of GMA and hence permits

efficacy of alkylation. On the contrary, the same alkylation achieves a lower extent in toluene as indicated by the negligible C=O absorption (Fig. 1c). It is rational that the long aliphatic chain of 1-amine would become contractive in toluene relative to in *n*-dodecane due to the differences between the two solvents in solubility parameters and the Kauri-Butanol numbers.[22] The coiled aliphatic chains would shield the terminal amino group from the epoxide group of GMA and therefore sterically retard the alkylation. Subsequent to the alkylation in the nonpolar medium, the resultant adduct product is subjected to polymerization *in-situ* to generate polymeric micelles in either *n*-dodecane or the diesel medium. The two polymer solids were separated from the micellar solutions P1 and P5 respectively as model samples for characterizations. The IR spectra of these two samples show the strongest aliphatic C-H stretch bands in range of 2800-3000 cm^{-1} and the characteristic carbonyl group of ester. In comparison, the control sample, PGMA (see Experimental Section), displays the asymmetrical epoxide-ring stretching peak at 906 cm^{-1} and the characteristic peaks of ester but far weaker C-H stretching peak as displayed in Fig. S1 (Supplementary Information). This spectral comparison supports the generation of the comb-like polymer structure. In addition to the IR evidence, the polymer sample separated from micellar solution P1, taken as an example, exhibits a stronger peak at chemical shift of δ= 1.11-1.93 ppm than PGMA (Fig. S2, Supplementary Information), which justifies as well the comb-like polymer structure. This assessment is similar to the NMR study reported by Leroux et. al.[23]

It is also curious about whether this comb-like polymer can be synthesized through attaching HDA or ODA to the PGMA backbone in a polar solvent. The alkylation was tested in both toluene and in MEK respectively. The comb-like chain formed in toluene precipitated when the alkylation reached a certain extent as a result of entanglement of the pendant aliphatic chains, which are weakly solvated in toluene as aforementioned. Alternatively, only a very low extent of alkylation in MEK could be achieved because the steric shielding of aliphatic chain to the 1-amino group is more severe in MEK than in toluene. The long alkyl tail of aliphatic amines has very low δ$_p$ (polarity cohesion parameter) and δ$_h$ (hydrogen bonding cohesion parameter) values. They are closer to the δ$_p$ and δ$_h$ of toluene (1.4 and 2 MPa$^{1/2}$) than to those of MEK (9 and 5.1 MPa$^{1/2}$).[24,25] Moreover, as PGMA is insoluble in *n*-dodecane, the alkylation cannot be carried out in this non-polar medium.

2. Colloidal behaviors for polymeric micellar solution

The micellization of the comb-like macromolecules in nonpolar medium was characterized by dynamic light scattering technique. No scattering was detected from the adduct monomer, GMA-HDA, in either *n*-dodecane or diesel because their sizes are below the instrument detection limit (< 2nm diameter). After polymerization, P(GMA-HDA) formed in *n*-dodecane, sample P1 (Table 1), reveals a size distribution of micelle centered at 15.9 nm and a polydispersity of 0.375, whereas the same polymer in diesel, sample P4, presents a distribution centered at 20.0 nm with a larger polydispersity of about 0.858 as shown in Fig. 2. The diesel contains aromatic hydrocarbons that have stronger affinity with the backbone of the polymer and cause micelles experience slight expansion. Both size distributions observed match the normal size range of micelles assembled by surfactants and amphiphilic polymers.[26] Regarding the particulate structure of micelles, a small amount of P1 solution was substantially diluted in *n*-heptane and a drop of liquid was sampled to conduct TEM examination. Sparse microcapsules with hollow structure were yet found in the sample and one of them was selected to present in Fig. 3a. The microcapsule is apparently far beyond the nano scale as identified by the light scattering measurement. This

variation happens likely because the original polymeric micelles undergo merging during dispersion in heptane. It is presumed that colloidal stability of the micellar solutions originates from comparable shape and size between the aliphatic side chains and the long-hydrocarbon-chain medium. Hence the dispersion in *n*-heptane largely impairs such size-dependent stabilization mechanism. As for the molecular weight of P(GMA-HDA), it cannot be accurately determined by size exclusion chromatography because driven by amphiphilic trait the polymer keeps particulate form in the eluent. Hence its average molecular weight of 927k must be overvalued (Fig. S3). Correspondingly, the PGMA sample, used as the reference of SEC, has an average molecular weight of 64k. In principle, PGMA should have a greater number average degree of polymerization than P(GMA-HDA) due to less steric hindrance to the polymerization.
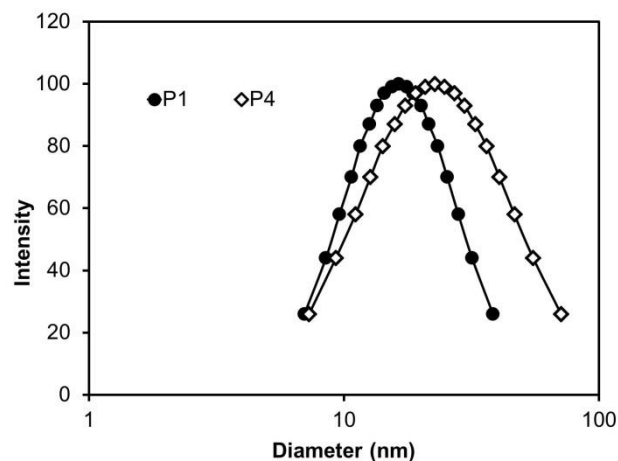

Fig. 2 Particles size distribution characterized by dynamic light scattering.
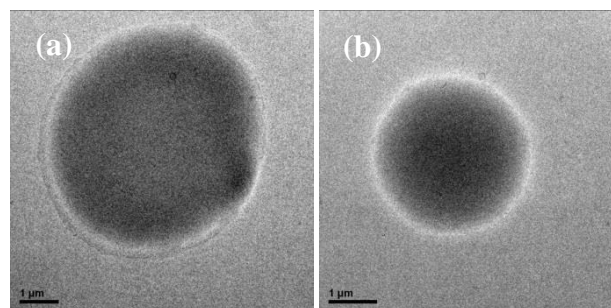
Fig. 3 Transmission electron micrograph of (a) a particle obtained from drying polymeric micellar solution P1, and (b) a particle obtained from a model diesohol, 20al/S$_e$4.

ARTICLE

3. Incorporation of methanol into the polymeric micellar solution

The dissolution capacity of methanol is a property related to the colloidal stability of the reverse polymer micelles (5 wt.%) in *n*-dodecane or the diesel. With the addition of alcohol into a polymeric micellar solution, a microemulsion is first produced since the resulting emulsion is optically transparent in which alcohol is distributed into the interior of individual micelles. Hence, the alcohol dissolution limit reflects the embryonic transition of the microemulsion to miniemulsion. It may be noted that pure *n*-dodecane has negligible methanol dissolution capacity compared with the presence of the comb-like polymer. In general, the *n*-dodecane-based microemulsions, S_m1, S_m2 and S_m3, exhibit greater than or at least comparable methanol dissolution capacities with the diesel-based emulsions, S_m4, S_m5, S_m6 and S_m8 (Table 2). The turbidity profiles of the S_m1, S_m2 and S_m3 microemulsions present close dissolution limits among them varying from 3.1 to 3.5 wt.% (Fig. 4). It is presumed that this narrow split reflect the structural similarity between the aliphatic moiety of the polymer and *n*-dodecane. S_m1 has a slightly larger capacity than S_m2 because the C_{16} aliphatic side-chain is more analogous to *n*-dodecane relative to the C_{18} counterpart. Regarding S_m3, it presents the lowest capacity in the *n*-dodecane medium because the polymer has a lower substitution density of aliphatic chains (C_{16}) than that used in S_m1. It may also note that the diesel-based microemulsions, S_m4 and S_m5, stabilized by the polymer with C_{16} and C_{18} side chains, respectively, exhibit flat turbidity profiles before the turbidity jump to greater than 1000 NTUs (Fig. 4 and Table 2). Compared with S_m1, the phase separation at the point just pass the dissolution limit is far more severe in S_m4 despite exactly the same polymeric stabilizer used in them. Such difference also happens in S_m2 vs. S_m5. Apparently *n*-dodecane defers the sudden collapse of microemulsion structure in contrast to the diesel likely owing to its rather complex composition.[27] This observation reveals a high demand of structural similarity between the polymer side-chain and the hydrocarbons of the dispersion phase for the stability of microemulsion accommodating highly hydrophilic methanol.
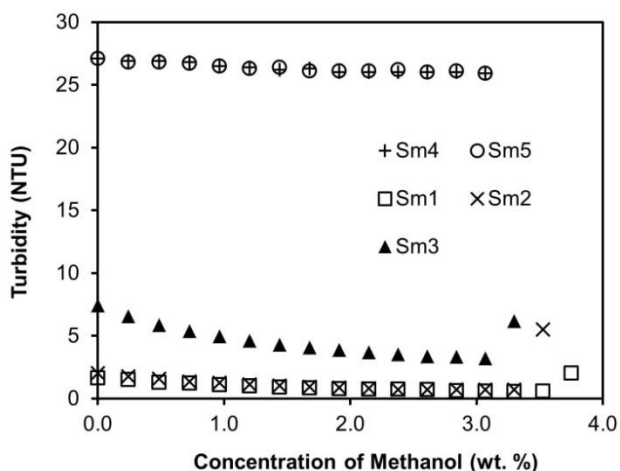
Fig. 4 The variation of turbidity with the addition of methanol into the five reverse polymeric micellar solutions where *n*-dodecane is the dispersion medium.

In addition, Fig. 5 presents the investigation on the methanol solubility in the four polymeric micellar solutions (P6 to P9) where the polymers contain PEG side chains besides the aliphatic chains (Table 1). Correspondingly, four microemulsions S_m6 to S_m9 exhibit the lower methanol dissolving limits than the preceding microemulsions by ca. 12-45%. In addition, both S_m7 and S_m9 become vulnerable when approaching to the limits because the polymers start precipitating out as sparse floc from the clear liquid, indicating not yet the broken of microemulsion. The flocculation could be attributed to the methanol-prompted coalescence of hydrophilic co-side-chain, PEG-360, end-capped by -OH group. On the contrary, the microemulsion state remains in S_m6 and S_m8 before reaching their methanol-dissolving limits because both emulsions are stabilized by the polymers bearing less hydrophilic PEG-300 co-side-chain end-capped by an -OCH_3 group. Similar to S_m4 and S_m5, the turbidity shoot up to *ca*. 1000 NTUs (Table 2) marks the methanol dissolving limits of S_m6 and S_m8. There is a lever rule between the size of hydrophilic core and the solvation extent of the aliphatic side chains in the dispersion medium. Hence, introduction of oligomeric PEG in the core of micelle in effect promotes instability as we observed from the above methanol dissolution examination.
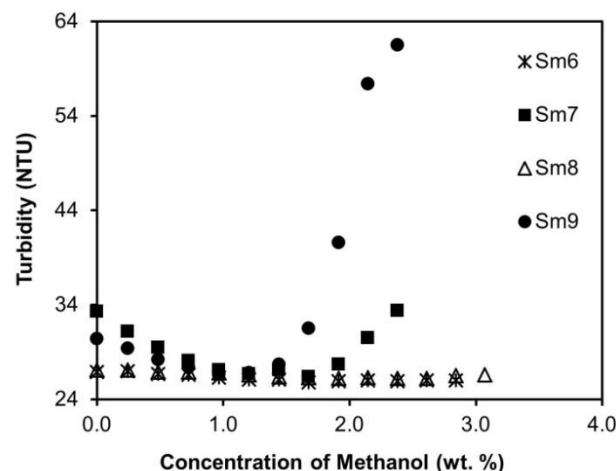
Fig. 5 The variation of turbidity with the addition of methanol into the four reverse polymeric micellar solutions (P6 to P9) where the diesel is the dispersion medium.

4. Examination of the ethanol dissolving limit in the diesel containing polymeric micelles

Ethanol is less hydrophilic than methanol and hence has a higher solubility limit (11.2%) in the diesel (Control 1, Table 3). Moreover, introducing a hydrophobic surfactant, Span® 80 (HLB =4.5), into the diesel brings about only a marginal improvement on ethanol solubility (Control 2). Interaction between ethanol and the hydrophilic moiety of Span® 80 might perturb the ordered assembly of the surfactant molecules. On this basis, the ethanol dissolution limit sustained by the P(GMA-HDA) polymer in the diesel was examined by varying its content. It turns out that the microemulsions S_e4 $S_e4\_2.5$ and S_e4_1 have their ethanol dissolution limits of 22.6, 16.3 and 12.7 wt.%, respectively (Table 3). Similarly, S_e5 shows an

ethanol-dissolution limit of 23.1%, which is also higher than the other two microemulsions of the same kind, $S_e5\_2.5$ and S_e5_1 (Fig. S4). Clearly, both S_e4 and S_e5 effectively enhance dissolution of ethanol in the diesel. In addition, these two microemulsions own similar ethanol dissolution limits despite the slightly different lengths of aliphatic side chains between the two polymeric emulsifiers. It is also noted that S_m4 and S_m5 display rather close turbidity readings to S_e4 and S_e5 before reaching their dissolution limits albeit the latter two microemulsions contain higher alcohol contents. As turbidity is a measure by the light scattering property of the emulsion particles, which depending on their size, shape, concentration and refractive index, the above observation implies that the disperse phases in $S_m\times$ and $S_e\times$ microemulsions possess similar interfacial structures and particle sizes, viz. the higher loadings of ethanol do not lead to apparently larger microemulsion particles. This happens likely because ethanol is structurally more analogous to the hydrophilic repeating unit of the polymer main chain, $-C(O)OCH_2CH(OH)CH_2NH-$, than methanol and a stronger association is incurred.

Correspondingly, a dry particle separated from S_e4 shows a denser interior than its external surface (Fig. 3b). The image implies a gel state formed through swelling of the polymer main chain by ethanol in the interior of microemulsion particles. Hence, a polymer matrix is left behind after the alcohol is removed. Moreover, the particle is also significantly larger than its micelle precursor, which could be attributed not only to ethanol swelling but also recombination of the polymer molecules during the dissolution of ethanol. It is deemed that the swelling of the hydrophilic polymer main chains by ethanol inside emulsion droplets offers a superior dissolution capacity over low-molecular-weight surfactant molecules since the swelling causes a gel structure, which is mechanically much more stable than liquid droplet. Furthermore, both S_e6 and S_e8 show slightly weaker ethanol-dissolution capabilities compared to S_e4 and S_e5. It is considered that too high an ethanol swelling degree of the hydrophilic PEG-300 side-chains would perturb with the balancing role of the aliphatic C_{16} and C_{18} side-chains in S_e6 and S_e8 as afore proposed. It is now clear that the structure of the comb-like polymer, the concentration of the polymeric micellar solution used to develop a microemulsion, and the composition of diesel affect the dissolution extent of ethanol in the diesel. Hence, performing an orthogonal experimental design in the future is essential in order to determine the optimal conditions for a stable ethanol-diesel blend with the maximum ethanol loading.

Pursuant to the above study on the introduction of ethanol into diesel, S_e4 and S_e5 prove to possess the maximum ethanol loading capacity amid the microemulsions listed in Table 3. Therefore, 20% ethanol loadings in these two formulated diesohol, labelled as $20al/S_e4$ and $20al/S_e5$, were formulated to carry out the following characterizations. In Fig. 6 the shear stress-shear rate (σ-$\dot{\gamma}$) relation of these two microemulsions and the two control samples, the diesel (Control 1) and micellar solution P4, were scrutinized. The two control samples manifest Newtonian fluid behavior. Micellar solution P4 has a slightly larger viscosity than the synergy diesel, i.e. 5.28 cp vs. 4.13 cp, due to the flocculation of polymeric micelles because of their out stretching aliphatic C_{16} chains into the continuous phase. Whereas the two microemulsions, $20al/S_e4$ and $20al/S_e5$, display lower σ with respect to $\dot{\gamma}$ than even the diesel. This phenomenon presumes that the microemulsion have a different interfacial structure than the micellar solution and a reduced density of the dispersion phase. In addition, both microemulsions exhibit almost identical two-stage σ-$\dot{\gamma}$ segments according to a slight decrease in slope (or viscosity), of which the first one ends at 75 s^{-1}. The capsuled ethanol might cause minor contraction of the pendant aliphatic side chains in diesel. From the perspective of application,

this measurement manifests the colloidal stability of microemulsion upon shearing within the range of testing.

The combustion measurement of the synergy diesel (Control 1 in Table 4) shows a gross calorific value (GCV) of 45825 kJ/kg, which is typical for commercial diesel. Inclusion of 5 wt.% polymeric micelles into it results in a slight reduction in GCV. If this amount of heat is approximately divided on the portion basis, the GCV of the polymer would be 2291 kJ/kg. To understand the combustion extent of the polymer in the diesel, the pyrolysis profiles of the above two samples were then assessed by TGA in air flow (Supplementary Information, Fig. S5). The results show that P4 displays basically the same combustion profiles as diesel. With respect to these two measurement values, $20al/S_e4$ exhibited a smaller GCV than that of P4. Taking the GCV of pure ethanol that is 29734 kJ/kg into account, the calculated combustion heat of $20al/S_e4$ should be 40430 kJ/kg based on the contribution of the three components by their corresponding portions. Hence, the measured GCV is greater than the calculated value by 6.5%. This improvement can be attributed to the oxygen brought in by ethanol. With regards to $20al/S_e5$, a slight reduction of the GCV by about 0.9% relative to $20al/S_e4$ was obtained. This observation suggests that too long the aliphatic side chains of comb-like polymer would become unfavorable to the combustion.
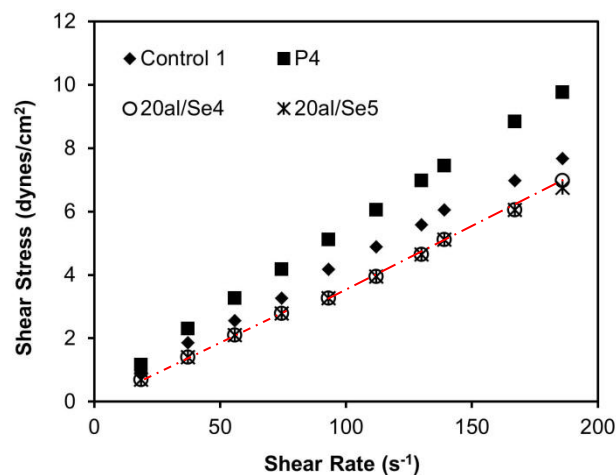

Fig. 6 The rheological characterization of the four samples as listed at room temperature.

Table 4 Model diesohol properties and combustion test

Sample	Emulsifier wt.%	Ethanol loading wt.%	Gross calorific value[a] (kJ/kg)	Viscosity (cP)[b]
Control 1	0	0	45825	4.13
P4	5	0	45425	5.28
20al/S_e4	5	20	43039	3.75
20al/S_e5	5	20	42648	3.63

[a]Based on ASTM D240-09. [b]Measured shear rate of 186 s^{-1}

Conclusions

The main findings of the present work are listed as follows:

1. Accomplishing the *in-situ* synthesis of a non-ionic amphiphilic polymer composed of hydrophilic main chain and long aliphatic side chains in a nonpolar solvent medium, which constitutes a micellar solution. This comb-like polymer is synthesized through the ring-opening alkylation of 1-alkyl (C_{16} or C_{18}) amine with glycidyl methacrylate and the subsequent free radical polymerization. The resulting polymeric micellar solution cannot be realized otherwise because the polymer if synthesized separately cannot be dissolved in the nonpolar solvent, typically saturated alkanes.

2. The resulting polymeric micellar solution possesses alcohol dissolution capability to form a microemulsion, whose stability is impaired to different extents by the presence of hydrophilic co-side-chain, e.g. polyethylene glycol, the non-aliphatic hydrocarbons in the non-polar medium, and the increase of hydrophilic trait of alcohol. The swelling of the hydrophilic backbone by alcohol to form a gel inside the microemulsion droplets upholds the diesohol formed.

3. The micellar solution using the ExxonMobil synergy diesel as the dispersion medium can effectively dissolve up to 23 wt.% ethanol. The gross calorific value measured in the model diesohol (diesel/ethanol/polymer = 75/20/5) exhibits an enhanced result that is attributed to the synergy of the ethanol and diesel.

Acknowledgements

Notes and references

[a] Department of Chemical and Biomolecular Engineering, National University of Singapore, 10 Kent Ridge Crescent, Singapore 119260, Singapore. E-mail: chehongl@nus.edu.sg

[b] Institute of Materials Research and Engineering, 3 Research Link, Singapore 117602, Singapore.

1   B. Brunekreef and S. T. Holgate, *Lancet*, 2002, **360**, 1233-1242.
2   R. O. McClellan, *Annu. Rev. Pharmacol. Toxicol.*, 1987, **27**, 279-300.
3   J. Campos-Fernández, J. M. Arnal, J. Gómez and M. P. Dorado, *Appl. Energy*, 2012, **95**, 267-275.
4   S. Kumar, J. H. Cho, J. Park and I. Moon, *Renewable Sustainable Energy Rev.*, 2013, **22**, 46-72.
5   A. C. Hansen, Q. Zhang and P. W. L. Lyne, *Bioresour. Technol.*, 2005, **96**, 277-285.
6   Z. Şahin and O. Durgun, *Energy Fuels*, 2009, **23**, 1707-1717.
7   A. Imran, M. Varman, H. H. Masjuki and M. A. Kalam, *Renewable and Sustainable Energy Rev.*, 2013, **26**, 739-751.
8   K. R. Gerdes and G. J. Suppes, *Ind. Eng. Chem. Res.*, 2001, **40**, 949-956.
9   M. Lapuerta, R. García-Contreras, J. Campos-Fernández and M. P. Dorado, *Energy Fuels*, 2010, **24**, 4497-4502.
10   E. Torres-Jimenez, M. S. Jerman, A. Gregorc, I. Lisec, M. P. Dorado and B. Kegl, *Fuel*, 2011, **90**, 795-802.
11   R. Chandra and R. Kumar, *Energy Fuels*, 2007, **21**, 3140-3414.
12   M. P. Ashok, *Energy Fuels*, 2010, **24**, 1822-1828.
13   E. J. Silva, M. E. D. Zaniquelli and W. Loh, *Energy Fuels*, 2007, **21**, 222-226.
14   Y. Reyes, D. A. G. Aranda, L. A. M. Santander, A. Cavado and C. R. P. Belchior, *Energy Fuels*, 2009, **23**, 2731-2735.
15   S. Fernando and M. Hanna, *Energy Fuels*, 2004, **18**, 1695-1703.
16   M. Lapuerta and O. Armas, *Energy Fuels*, 2009, **23**, 4343-4354.
17   O. Armas, M. Gómez, E. J. Barrientos and A. L. Boehman, *Energy Fuels*, 2011, **25**, 3283-3288.
18   P. Kwancharoen, A. Luengnaruemitchai and S. Jai-In, *Fuel*, 2007, **86**, 1053-1061.
19   S. Lebedevas, G. Lebedeva, V. Makareviciene, P. Janulis and E. Sendzikiene, *Energy Fuels*, 2009, **23**, 217-223.
20   N. Yilmaz, *Energy*, 2012, **40**, 210-213.
21   A. P. Richez, H. N. Yow, S. Biggs and O. J. Cayre, *Prog. Polym. Sci.*, 2013, **38**, 897– 931.
22   G. Knothe and K. R. Steidley, *Ind. Eng. Chem. Res.*, 2011, **50**, 4177–4182.
23   H. Gao, M. Elsabahy, E. V. Giger, D. Li, R. E. Prud'homme and J-C. Leroux, *Biomacromolecules*, 2010, **11**, 889–895.
24   J. Jang, V. H. Pham, S. H. Hur and J. S. Chung, *J. Colloid Interface Sci.*, 2014, **424**, 62-66.
25   C. M. Hansen, *Hansen Solubility Parameters: A User's Handbook*, CRC Press, Boca Raton, FL, 2nd edn., 2000.
26   T. S. Kale, A. Klaikherd, B. Popere and S. Thayumanavan, *Langmuir*, 2009, **25**, 9660-9670.
27   S. Puri, A. Gupta, H. Dekka, M. Vanmamalai, A. Jha, R. Malhotra and N. Raje. *US Pat.*, 20060277819 A1, Dec 14, 2006.

RSC Advances Accepted Manuscript